Carcinogenesis, 2022, **43**, 1137–1148
https://doi.org/10.1093/carcin/bgac089
Advance access publication 10 November 2022
Original Article

Original Article

Inflammation as a chemoprevention target in asbestos-induced malignant mesothelioma

Yuwaraj Kadariya[1], Eleonora Sementino[1], Ujjawal Shrestha[1], Greg Gorman[2], Jonathan M. White[3], Eric A. Ross[4], Margie L. Clapper[5], Nouri Neamati[6], Mark Steven Miller[7] and Joseph R. Testa[1,*]

[1]Cancer Signaling and Microenvironment Program, Fox Chase Cancer Center, Philadelphia, PA, 19111, USA
[2]Department of Pharmaceutical, Social and Administrative Sciences, Samford University McWhorter School of Pharmacy, Birmingham, AL, 35229, USA
[3]Division of Pharmaceutical Sciences, MRIGlobal, Kansas City, MO, 64110, USA
[4]Biostatistics and Bioinformatics Facility, Fox Chase Cancer Center, Philadelphia, PA, 19111, USA
[5]Cancer Prevention and Control Program, Fox Chase Cancer Center, Philadelphia, PA, 19111, USA
[6]Department of Medicinal Chemistry, University of Michigan, Ann Arbor, MI, 48109, USA
[7]Division of Cancer Prevention, National Cancer Institute, 9606 Medical Center Drive, Rockville, MD, 20850, USA
[*]Corresponding author: Tel: +1 215-728-2610; Fax: 1 215-214-1737;Email: joseph.testa@fccc.edu

Abstract

Malignant mesothelioma (MM) is an incurable cancer of the serosal lining that is often caused by exposure to asbestos. Therefore, novel agents for the prevention and treatment of this disease are urgently needed. Asbestos induces the release of pro-inflammatory cytokines such as IL-1β and IL-6, which play a role in MM development. IL-6 is a component of the JAK-STAT3 pathway that contributes to inflammation-associated tumorigenesis. Glycoprotein 130 (gp130), the signal transducer of this signaling axis, is an attractive drug target because of its role in promoting neoplasia via the activation of downstream STAT3 signaling. The anticancer drug, SC144, inhibits the interaction of gp130 with the IL-6 receptor (IL6R), effectively blunting signaling from this inflammatory axis. To test whether the inflammation-related release of IL-6 plays a role in the formation of MM, we evaluated the ability of SC144 to inhibit asbestos-induced carcinogenesis in a mouse model. The ability of sulindac and anakinra, an IL6R antagonist/positive control, to inhibit MM formation in this model was tested in parallel. Asbestos-exposed *Nf2*$^{+/-}$*;Cdkn2a*$^{+/-}$ mice treated with SC144, sulindac or anakinra showed significantly prolonged survival compared to asbestos-exposed vehicle-treated mice. STAT3 activity was markedly decreased in MM specimens from SC144-treated mice. Furthermore, SC144 inhibited STAT3 activation by IL-6 in cultured normal mesothelial cells, and *in vitro* treatment of MM cells with SC144 markedly decreased the expression of STAT3 target genes. The emerging availability of newer, more potent SC144 analogs showing improved pharmacokinetic properties holds promise for future trials, benefitting individuals at high risk of this disease.

Graphical Abstract

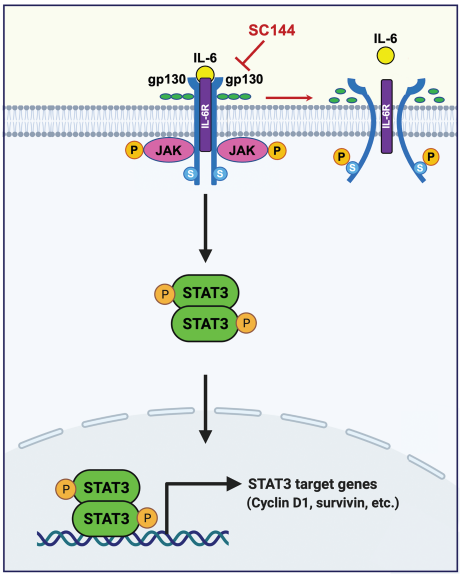

Received: July 5, 2022; Revised: October 11 2022; Accepted: November 7, 2022

Introduction

Malignant mesothelioma (MM) is a fatal cancer that arises from the serosal lining of pleural, peritoneal and pericardial cavities. Patients with MM typically present with advanced disease that is often surgically inoperable and refractory to standard therapy. Exposure to asbestos, particularly amphibole fibers, is the main cause of MM (1). More than 3000 cases of MM are diagnosed in the USA each year, and countries such as Russia, India and China, where asbestos is still used with little regulation, are expected to show dramatic increases in MM incidence and mortality in future years (2). Consequently, innovative approaches to the prevention and treatment of this incurable disease are urgently needed.

Asbestos carcinogenicity has been linked to its ability to cause the release of pro-inflammatory cytokines and growth factors, as well as the generation of mutagenic oxygen radicals from exposed mesothelial cells and nearby macrophages (2). Early work on mice exposed to asbestos demonstrated that activated macrophages recruited to the mesothelial lining interact with these carcinogenic fibers [reviewed in (3)]. As a result of the accumulation of macrophages, the mesothelial lining is exposed to pro-inflammatory cytokines, such as IL-1β and TNF-α, which can act in concert with asbestos to transform mesothelial cells, suggesting that inflammation directly contributes to MM formation. In addition to IL-1β and TNF-α, other inflammatory cytokines such as IL-6 are released from mesothelial cells and macrophages following exposure to asbestos (4,5). The NLRP3 (previously dubbed NALP3) inflammasome has been shown to mediate inflammation and IL-1β production from macrophages in response to asbestos (6). In both untreated and asbestos-exposed mice with heterozygous knockout of the *Asc* gene, which encodes a component of the inflammasome, decreased levels of IL-1β and IL-6 were found in the serum and peritoneal lavage fluid when compared to levels in wild-type littermates (4).

Human MMs show frequent mutations and/or losses of several tumor suppressor genes, including *CDKN2A* and *NF2*. Mice heterozygous for murine homologs of these genes ($Nf2^{+/-}$;$Cdkn2a^{+/-}$ mice) develop highly aggressive MMs with nearly 100% penetrance and short latency (median, 22.6–24 weeks) when injected chronically with crocidolite, making this model highly amenable to preclinical studies (4,7). Previous studies by this group indicated that treatment with the IL-1β receptor antagonist anakinra significantly delayed the onset and progression of MM in this genetically engineered mouse (GEM) model (4). These findings suggest that inflammation caused by asbestos deposition in or near mesothelial tissue is a key factor contributing to MM development and that such inflammatory processes might serve as viable early intervention targets for the delay/prevention of this incurable form of cancer.

To date, the role of the cytokine IL-6 in MM development and progression has not yet been formally tested. IL-6 and STAT3 play key roles in certain malignancies such as ovarian cancer (8). Glycoprotein 130 (gp130) is the signal transducer of this signaling axis and is an attractive drug target because of its role in promoting tumor progression via the activation of downstream STAT3 signaling. IL-6 acts by binding to the IL-6R on target cells, and then the IL-6/IL-6 receptor (IL-6R) complex recruits gp130, which thereby boosts its dimerization and subsequent activation of STAT3 signaling via STAT3 phosphorylation by JAK. Upon phosphorylation, STAT3 forms dimers that translocate to the nucleus, where they regulate the transcription of target genes.

Neamati et al. discovered a novel class of anticancer compounds known as quinoxaline hydrazides that showed remarkable potency in a panel of carcinoma cell lines. The lead compound, SC144, also exhibited significant *in vivo* efficacy in mouse xenograft models of human ovarian cancer (8). SC144 was found to bind to gp130 and inhibit its interaction with IL-6R, effectively blunting signaling from the inflammatory axis (8). When SC144 binds gp130, it induces phosphorylation and conformational changes that decrease the activity of gp130, and it can cause deglycosylation of gp130 and degradation of gp130 at higher drug levels (10 μM). As a result, STAT3 phosphorylation and nuclear translocation are abolished, which leads to inhibited expression of downstream STAT3 target genes. Moreover, oral administration of SC144 delayed tumor growth in a mouse xenograft model of human ovarian cancer without causing significant toxicity to normal tissues (8).

The goal of this study was to assess the ability of SC144 to inhibit MM in an asbestos-induced GEM model. The ability of sulindac, a non-steroidal anti-inflammatory drug (NSAID), and anakinra, an IL-1 receptor antagonist used as a positive control, to prevent or delay the progression of MM in this model was tested in parallel. The results from this preclinical study have implications for future trials in individuals at high risk of MM development, such as asbestos workers.

Materials and methods

Animals

$Cdkn2a^{+/-}$ (01XB2, FVB/N.129-Cdkn2atm1Rdp) mice, which have a heterozygous deletion of exon 2 of *Cdkn2a* (encoding portions of both p16Ink4a and p19Arf), were obtained from the Mouse Models of Human Cancers Consortium. $Nf2^{+/-}$ (129 Sv) mice were obtained from Drs. Tyler Jacks (MIT, Cambridge, MA) and Andrea I. McClatchey (Massachusetts General Hospital, Charleston, MA), and these mice were later backcrossed multiple generations to FVB/N mice. $Cdkn2a^{+/-}$ mice were crossed with $Nf2^{+/-}$ mice to obtain doubly heterozygous $Cdkn2a^{+/-}$;$Nf2^{+/-}$ mice on an FVB/N genetic background, which were used for all experiments. Animals were maintained on a Teklad TD.00588 Global 18% Protein Rodent Diet, Envigo, which was used as the basal chow. All *in vivo* experiments were performed in accordance with guidelines of the NIH Guide for the Care and Use of Laboratory Animals and a protocol approved by members of Fox Chase Cancer Center's IACUC.

Asbestos and pharmaceuticals

The required amount of UICC grade crocidolite (SPI Supplies) was baked overnight at 150°C under a mercury pressure of 15 mm. The following day, a stock solution of crocidolite (1.6 mg/ml) was prepared in Hanks balanced salt solution (HBSS). Each dose of crocidolite consisted of 800 μg of fibers in 0.5 ml HBSS. Anakinra (Kineret, Amgen), a human recombinant IL-1R antagonist, was dissolved and diluted in a citrate buffer (100 μg/0.1 mL). Anakinra was administered intraperitoneally (i.p.) at a final concentration of 5 mg/kg body weight (100 μg/injection per adult mouse weighing ~20 g) 6 h before the first asbestos injection and every third day after each asbestos injection at the same concentration. In

parallel, control *Nf2*$^{+/-}$;*Cdkn2a*$^{+/-}$ mice were injected i.p. with vehicle (100 µL citrate buffer).

Sulindac was delivered orally in a drug-infused chow (150 ppm sulindac) in an 18% Protein Rodent Diet (Envigo). The average dose of sulindac consumed per day by each mouse was estimated to range from 22.5 to 30 mg/kg of body weight (human equivalent dose = 109–146 mg/kg). Sulindac-infused chow was administered to mice 24 h prior to the first asbestos injection and then ad libitum for the remainder of the experiment. Sulindac-infused chow was stored at 4–8°C, and the chow was replaced in the cages every week to ensure the stability of the compound in the chow.

SC144 (Supplementary Figure 1) was synthesized using the method described by Grande et al. (9). In this procedure, SC144 was obtained as a hydrochloride salt (MRIGlobal lot 13667-51, purity 97.2%). To produce the free base, the material was neutralized using sodium bicarbonate and extracted into an organic solvent, followed by solvent removal and drying (MRIGlobal lot 13667-54, purity 97.4%). Purity was determined by the HPLC-peak area percentage, and identity was confirmed by 1H NMR. The water used throughout the experiment was purified by reverse osmosis.

Pilot studies have revealed that, similar to other quinoxaline hydrazides, SC144 is characterized by low solubility and low bioavailability. Prior to testing for the preclinical MM study, the solubility and stability of SC144 were evaluated using several vehicles, and Labrafil M 1944, a liquid non-ionic water-dispersible surfactant, was determined to be an effective vehicle for drug delivery. In pilot studies, SC144 formulated in Labrafil and delivered orally (150 mg/kg SC144 formulated in a 50:50 ratio of Labrafil M 1944 in citrate buffer, pH 4.0) showed sustained elevated drug concentration levels in the plasma with minimal variation among experimental animals compared to the other vehicles tested (Supplementary Methods; Supplementary Figure 2, Supplementary Tables 1 and 2). Based on the data shown in Supplementary Table 1, SC144 formulations were prepared as follows for the long-term preclinical study: Labrafil: citrate (L:C) buffer (50:50) at concentrations of 15 and 30 mg/ml (75 and 150 mg/kg doses, respectively; estimated human equivalent doses = 6.075 and 12.15 mg/kg, respectively). A daily dose of ~100 µL of either the 15 mg/ml formulation (75 mg/kg group) or the 30 mg/kg formulation (150 mg/kg group) was administered orally to each mouse, with the actual volume adjusted based on the weight of each animal. Control mice were orally administered 100 µL of L:C (50:50) solution (vehicle).

Chemoprevention studies

Chemoprevention study I consisted of three experimental groups injected with asbestos, with 25 mice in each arm: (i) basal chow, with mice injected i.p. with phosphate-buffered saline (PBS); (ii) basal chow infused with 150 ppm sulindac and (iii) basal chow, with mice injected i.p. with 5 mg/kg body weight anakinra.

Mice of approximately equal numbers of both genders, 8–10 weeks of age, were injected i.p. with 800 µg of crocidolite every 21 days for a total of four injections (total = 3.2 mg/mouse) using a 25-G needle per our usual method (10). SC144 and vehicle (L:C) were administered to the mice 6 h before the first asbestos injection and then Monday through Friday (for oral gavage) throughout the remainder of the experiment. Anakinra was injected intraperitoneally (i.p.) 24 h before the first asbestos injection. After each asbestos injection, anakinra was administered every third day at the same dose. Sulindac-infused chow was administered 24 h prior to the first asbestos injection, and then *ad libitum* for the remainder of the experiment.

For the SC144 study (chemoprevention study II), approximately equal numbers of male and female mice 8–10 weeks of age (22–29 per group) were assigned to four experimental groups: (i) no asbestos + L:C control; (ii) asbestos + L.C. control; (iii) asbestos + SC144 (75 mg/kg in L:C) and (iv) asbestos + SC144 (150 mg/kg in L:C). All mice were serially injected i.p. with crocidolite as described above. Vehicle or an SC144 in L:C buffer (50:50) solution was administered orally to separate groups of mice. Oral gavage of SC144 drug or vehicle was started on the same day as the first crocidolite injection and continued for 5 days a week (Monday through Friday, with a weekend drug holiday) until euthanasia.

Detection of tumors

All mice were examined daily and sacrificed upon detection of abdominal bloating, weight loss > 10%, labored breathing, severe lethargy, or when palpable or visible masses arose. At that point, the mice were euthanized via CO_2 asphyxiation, followed by cervical dislocation. All internal organs, including lymph nodes, were collected, fixed in formalin and subjected to histopathological assessments. Although all mice underwent complete necropsies, detailed analyses of the peritoneum, pleura, diaphragm and pericardium to detect MM were the highest priority. When available, ascitic fluid was collected to generate tumor cell cultures that were grown in Dulbecco's modified eagle medium (DMEM) supplemented with 10% fetal bovine serum (FBS).

Histopathology and immunohistochemistry

Formalin-fixed/paraffin-embedded (FFPE) samples were cut into 5-µm sections and mounted onto positively charged microscope slides. Hematoxylin and eosin (H&E)-stained sections were used for the histopathological evaluation. FFPE sections were subjected to heat-induced epitope retrieval for immunohistochemistry (IHC). Endogenous peroxidase activity was quenched with 3% hydrogen peroxide, and non-specific protein binding was blocked with goat serum prior to incubating the sections with primary monoclonal antibodies. To differentiate MM from adenocarcinoma, IHC was performed for various markers of MM, including mesothelin (Santa Cruz Biotechnology), WT1 (Cell Signaling Technology) and Troma 1 (a marker of cytokeratin) (Sigma). Phospho (P)-specific AKT, ERK, STAT3 and JNK antibodies (Cell Signaling Technology) were used to assess the activity of the downstream effectors of IL-1β and IL-6 signaling. To assess IHC staining for nuclear Ki67, two to three sections from MMs (six to seven mice per arm) were incubated overnight with primary anti-Ki67 monoclonal antibodies, followed by treatment with biotinylated goat anti-rat IgG. Detection and visualization of the antibody complexes were carried out using the labeled streptavidin-biotin system (Dako) and the chromogen 3,3′-diaminobenzidine. Murine samples previously shown to express high levels of each of the investigated proteins were used as positive controls. As a negative control, the primary antibody was replaced with a normal mouse/rabbit IgG to confirm the absence of specific staining. For quantitative image analysis, immunostained slides were

scanned using an Aperio Scan Scope CS scanner and image viewer software. The proliferative index of individual Ki67-stained tumor sections was quantified using Aperio's nuclear V9 algorithm.

Immunoblotting

For immunoblotting, protein lysates were prepared as previously described (7). Lysates (30–50 µg/sample) were loaded onto polyacrylamide gels, transferred to nitrocellulose membranes (1620115, Bio-Rad, Hercules, CA), and probed with the primary antibodies listed in Supplementary Table 3. Anti-rabbit (45-000-682, 1:5000) and anti-mouse secondary antibodies (45-000-679, 1:5000–50,000 depending on the primary antibody) were purchased from Fisher Scientific (Waltham, MA). Immunoblots were imaged using Immobilon Western Chemiluminescent HRP Substrate (ECL) (WBKLS0500, MilliporeSigma, Ontario, Canada).

Immunoblot analysis of mouse mesothelial and MM cells treated *in vitro* with SC144

Primary non-malignant mesothelial cells (NMCs) were isolated from the mesothelial lining of 10- to 12-week-old *Nf2*$^{+/-}$;*Cdkn2a*$^{+/-}$ mice and wild-type littermates by adding trypsin (0.25% trypsin-EDTA, Gibco, #25200-056) to the peritoneal cavity of euthanized mice. The resulting cells were seeded into six-well plates (Thermo Fisher BioLite 6-well Multidishes, #130184) and grown to confluence in a medium supplemented with 15% FBS. Early-passage (p. 4) *Nf2*$^{+/-}$;*Cdkn2a*$^{+/-}$ NMC 701 and 704 were cultured overnight in a medium containing 1% FBS and 40 µM SC144. The following morning, the medium was replenished with fresh SC144 for another 4 h, and recombinant mouse IL-6 (recombinant mouse IL-6 protein, #406-ML-005, R&D Systems, Minneapolis, MN) at 100 ng/ml was added for the final 15 min before harvesting the cells to prepare lysates for immunoblot analyses.

MM cells obtained from the ascitic fluid of three vehicle-treated MM mice (MM 166, MM 174 and MM 364) were seeded in six-well plates. When the cells reached 60% confluency, they were treated with different concentrations of SC144 (0, 10, 20 and 40 µM) for 72 h in DMEM supplemented with 10% FBS. After 72 h, cells were collected for immunoblot analysis. The NMC and MM cells used in this study were cultured for several passages only, and all of these cell cultures were genotyped prior to use in experiments to authenticate their origin from the corresponding wild-type and *Nf2*$^{+/-}$;*Cdkn2a*$^{+/-}$ mice from which each was derived.

Immunoblot analysis of human mesothelial and MM cells treated *in vitro* with SC144

Most of the pleural MM cell lines used in this study were generated as reported previously (11). LP9, a normal human mesothelial cell strain, was obtained from Coriell Institute, (Camden, NJ; AG07086). Other MM cell lines, cell culture media, SC144 treatments and immunoblot analysis are described in the Supplementary Methods and figure legends.

Cell viability assays

For each human MM cell line tested, cells were seeded onto 96-well plates at a density of 1000 cells per well. After 24 h, the MM cells were washed with PBS and treated with different concentrations of SC144 (0.078–20 µM) in RPMI1640 supplemented with 0.5% FBS or with vehicle control for 96 h. Cell viability was determined using the MTS assay (Promega, Madison, WI; #G3582). MTS reagent was added to each well, and absorbance was determined at 490 nm as a read-out of cell viability.

Colony formation assay

Human MM cell lines were trypsinized, counted and then seeded in six-well plates in triplicate at a density of 10 000 cells/well. After 24 h, serial dilutions of SC144 (0, 0.625, 1.25 or 2.5, 5 and 10 µM) were added to the culture medium supplemented with 0.5% FBS, and the cells were incubated for 7 days to allow colonies to form. Subsequently, the colonies were stained using a Diff-Quik stain kit (Siemens, Munich, Germany).

Statistical analysis

Log-rank tests were used to assess the statistical significance of differences among mouse treatment groups with respect to tumor incidence and time to MM formation. The failure time for these analyses was defined as the age at the time of tumor detection. Animals that died of causes other than MM or unknown causes leading to autolysis were considered censored at the time of death. Survival comparisons were made between asbestos-exposed cohorts of *Nf2*$^{+/-}$;*Cdkn2a*$^{+/-}$ mice treated with SC144, sulindac, anakinra and vehicle (control). Statistical assessments were performed using the Biostatistics and Bioinformatics Facility at Fox Chase Cancer Center.

Results

Treatment of asbestos-exposed *Nf2*$^{+/-}$;*Cdkn2a*$^{+/-}$ mice with sulindac or anakinra resulted in significantly prolonged survival compared to that of asbestos-exposed vehicle-treated littermates (Figure 1A; Table 1). Moreover, these therapeutic benefits were observed without significant weight loss in treated mice over time.

Next, we tested whether SC144 could prevent or delay the progression of asbestos-induced MM in *Nf2*$^{+/-}$;*Cdkn2a*$^{+/-}$ mice in a two-dose study of SC144 suspended in L:C buffer (Supplementary Table 4). The median survival and survival curves of asbestos-exposed animals treated with vehicle or two different doses of SC144 (75 and 150 mg/kg) are presented in Table 1 and Figure 1B, respectively. The median survival of animals in the 150 mg/kg SC144 treatment group was 23.8 weeks compared to 19.4 weeks in the vehicle control group, which was statistically significant ($P < 0.0001$). Treatment with 75 mg/kg SC144 resulted in a median survival of 23.0 weeks, which also achieved statistical significance compared to the vehicle-treated group ($P < 0.001$). Moreover, mice administered SC144 did not show any signs of weight loss or other evidence of toxicity.

H&E staining and IHC were performed for all tumors to confirm the histological diagnosis of MM. Representative examples of H&E and IHC staining for Ki67 are shown in Figure 2A. Ki67 staining was used to examine the cell proliferation index of individual tumors from SC144-treated and vehicle-treated mice. The mean cell proliferation index was significantly diminished in MMs from SC144-treated mice compared to vehicle-treated mice ($P = 0.013$, two-sided Wilcoxon rank sum test) (Figure 2B). IHC staining

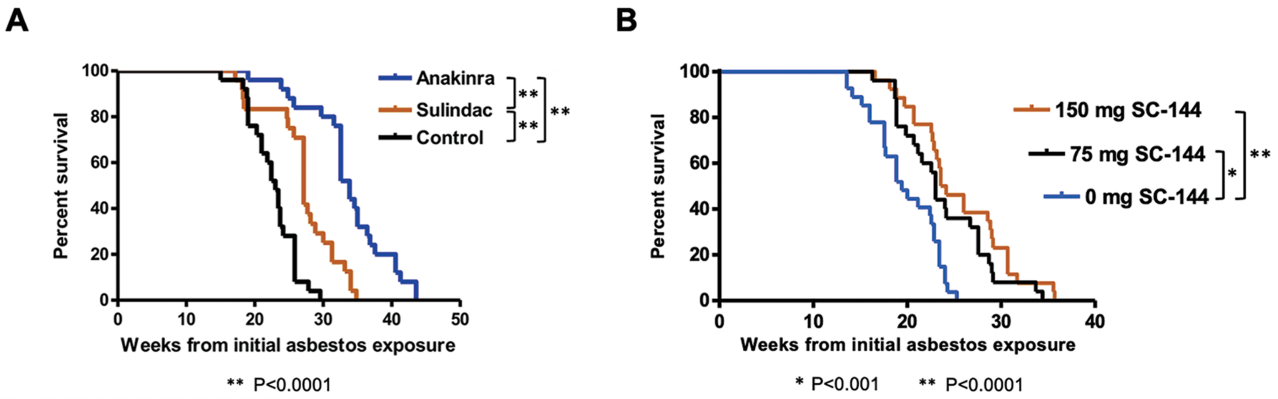

Figure 1. Kaplan–Meier survival curves of asbestos-exposed *Nf2*$^{+/-}$;*Cdkn2a*$^{+/-}$ mice treated with anti-inflammatory agents. (**A**) Survival curves of mice treated with sulindac, anakinra or vehicle (citrate buffer). (**B**) Survival curves of mice treated with vehicle control (Labrafil:citrate buffer, L:C), 75 mg/kg SC144, or 150 mg/kg SC144. The outcome was time to death due to MM. Animals that were MM-free when they expired were censored at the time of death. Statistical significance between experimental groups was assessed using the log-rank test.

Table 1. Median survival of asbestos-exposed *Nf2*$^{+/-}$;*Cdkn2a*$^{+/-}$ mice treated with sulindac, anakinra or SC144 in two separate experiments

Treatment group	No. mice	No. with MM (%)	Median survival (weeks)	*P* value[a]
Control[b]	25	25 (100%)	23.0	
Sulindac	24[c]	23 (95.8%)	27.1	$P < 0.0001$ (vs. control)
Anakinra	25	23 (92.0%)	33.9	$P < 0.0001$ (vs. control); $P < 0.0001$ (vs. sulindac)
Control[d]	28	27 (96.4%)	19.4	
SC144 75 mg/kg	28	25 (89.3%)	23.0	$P < 0.001$ (vs. control)
SC144 150 mg/kg	29	26 (89.7%)	23.8	$P < 0.0001$ (vs. control)

[a]Differences in median survival were calculated using log-rank test.
[b]Vehicle = citrate buffer.
[c]One mouse died.
[d]Vehicle = Labrafil:citrate buffer.

of MMs from SC144-treated mice with a P-Stat3 antibody was very weak compared with that of MMs from vehicle-treated animals (Figure 2C). Consistent with these IHC findings, immunoblot analyses demonstrated robust expression of P-Stat3 in MMs from vehicle-treated mice, but distinctly diminished expression in MMs from SC144-treated mice; the expression of total Stat3 was markedly reduced in tumors from mice in the 150 mg/kg SC144-treatment group (Figure 3A). As shown in Figure 3B, SC144 also inhibited the activation of Stat3 by IL-6 in cultured NMCs isolated from the mesothelial lining of *Nf2*$^{+/-}$;*Cdkn2a*$^{+/-}$ mice.

To confirm that the anti-inflammatory compound SC144 inhibits the IL-6/JAK-STAT3 pathway, we performed immunoblot analyses on three randomly selected MM cell cultures of ascitic fluid from vehicle-treated MM mice (MM 166, MM 174 and MM 364) grown *in vitro* in the absence or presence of SC144 at several different concentrations (10, 20 or 40 μM) for 72 h. Immunoblotting demonstrated markedly diminished expression of P-Stat3 with increasing doses of SC144 and abrogated the expression of two downstream effectors, cyclin D1 and survivin (Figure 4A). A diagram depicting the effect of SC144 on the IL-6/JAK-STAT3 pathway is shown in Figure 4B.

To determine if SC144 has a similar inhibitory effect on IL-6/JAK-STAT3 signaling in human mesothelial cells, we performed immunoblot analyses on both LP9, a non-malignant mesothelial cell strain, and several human MM cell lines. Immunoblot analyses demonstrated that SC144 inhibited IL-6-induced activation of STAT3 and the expression of two protein products (cyclin D1 and survivin) of STAT3 target genes in LP9 mesothelial cells (Figure 5A). Immunoblotting also revealed that SC144 inhibited STAT3 activity and cyclin D1 expression in a dose-dependent manner in human MM cell lines, two of which are shown in Figure 5A. SC144 was also found to inhibit MM cell viability and colony formation in a dose-dependent manner (Figure 5B, C).

Discussion

Asbestos exposure has been linked to inflammation, which is thought to play a significant role in MM development (4,5). Consistent with this idea, we demonstrated here that treatment with several different anti-inflammatory agents delays

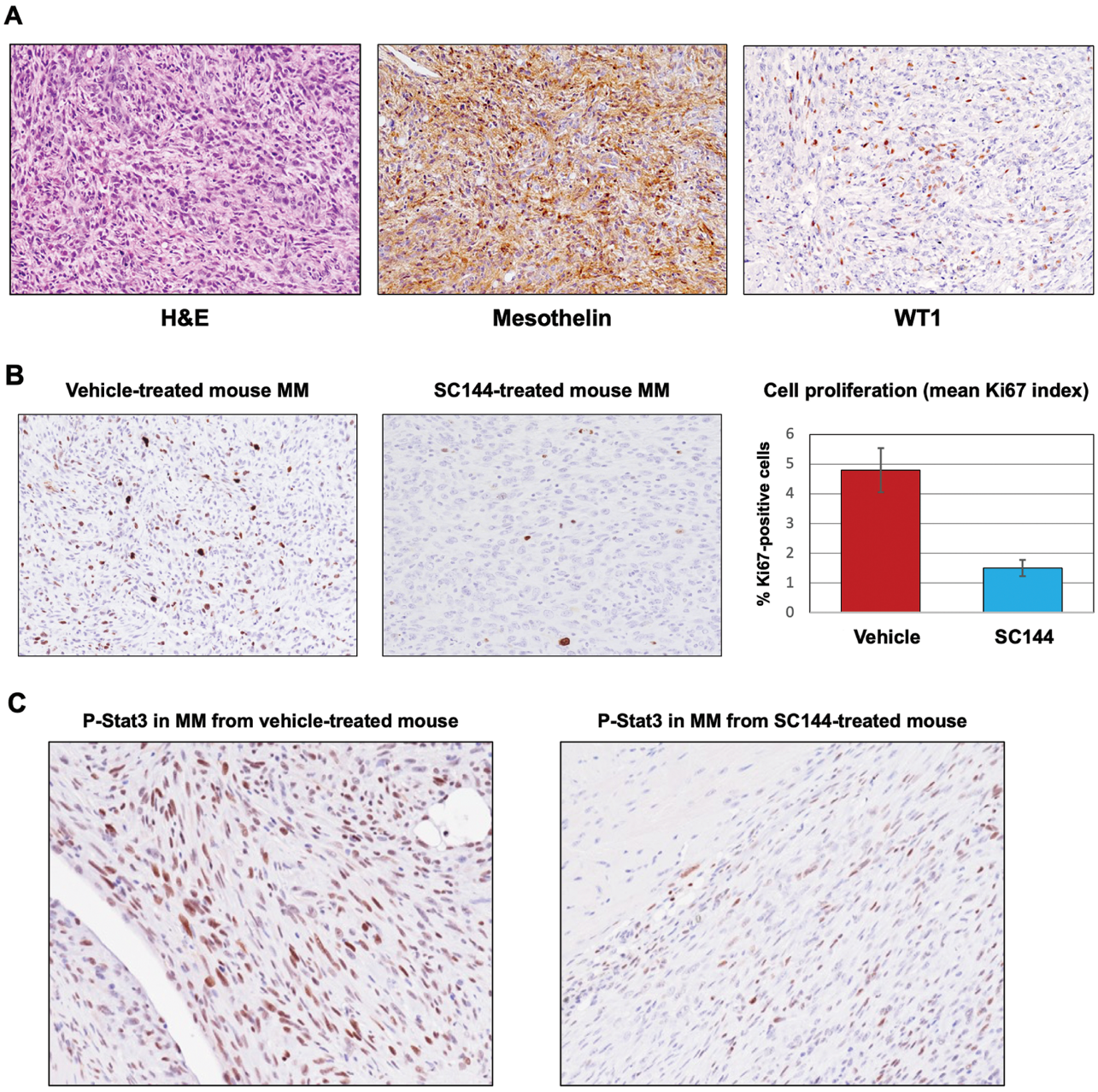

Figure 2. Histopathological and immunohistochemical analyses of representative MMs from asbestos-injected *Nf2*$^{+/-}$;*Cdkn2a*$^{+/-}$ mice. (**A**) Histopathological assessment of representative MM from asbestos-injected *Nf2*$^{+/-}$;*Cdkn2a*$^{+/-}$ mouse. Left panel, H&E staining; middle, mesothelin staining and right, WT1 staining. (**B**) Left and middle panels, Ki67 staining of MMs from vehicle-treated and SC144-treated *Nf2*$^{+/-}$;*Cdkn2a*$^{+/-}$ mice, respectively. Right panel, bar graph depicting mean Ki67 proliferation index in MMs from the two mouse treatment groups ($n = 5$). Error bars indicate the standard error of the means (SEM). (**C**) Immunohistochemical staining with phospho (P)-Stat3 antibody in representative MMs from vehicle-treated (***left panel***) and SC144-treated (***right***) mice. The original magnification of all histopathological images was ×200.

the onset of asbestos-induced MM in an experimental mouse model.

Treatment of asbestos-exposed *Nf2*$^{+/-}$;*Cdkn2a*$^{+/-}$ mice with sulindac, an NSAID that inhibits cyclooxygenase 1 and 2 (COX-1/2), significantly prolonged survival compared to that observed in asbestos-exposed *Nf2*$^{+/-}$;*Cdkn2a*$^{+/-}$ mice treated with the vehicle control. Sulindac undergoes reversible reduction by colonic bacteria to form sulindac sulfide, a potent inhibitor of COX-1/2 enzymatic activity. In addition, sulindac and sulindac sulfide are irreversibly oxidized to sulindac sulfone, which lacks COX-1 and COX-2 inhibitory activities (12). In a long-term (mean, 7.4 years) chemoprevention study of patients with adenomatous polyposis coli, who were at high risk of developing colorectal cancer (CRC), sulindac was found to be effective and safe (13). Advanced adenomas were found in 8 of 54 patients within the first 5 years of chemoprevention, and none of the patients developed the desmoid disease. In another study, the anti-tumor effects of sulindac sulfone were documented in rodent models of various cancers, such as mammary, lung and prostate cancers (12). However, long-term use of sulindac and other NSAIDS is not recommended because of the potentially fatal toxicities associated with COX inhibition. The mechanism responsible for the anticancer activity

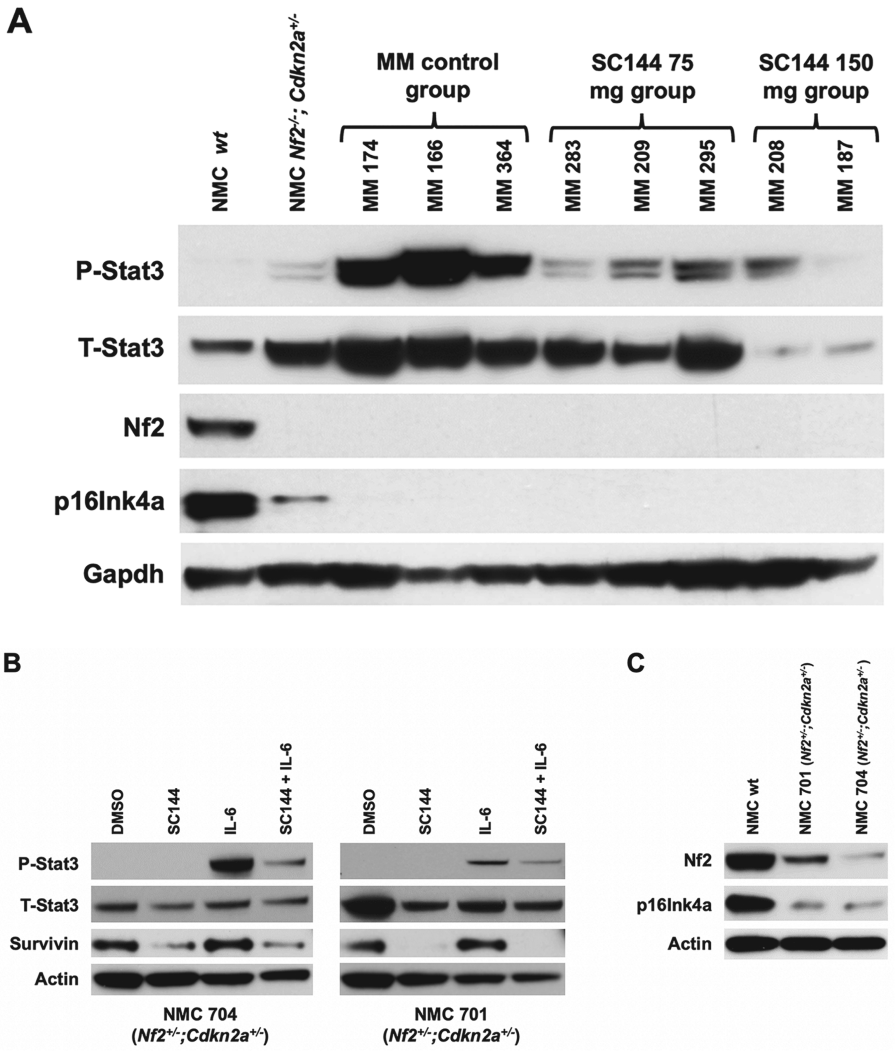

Figure 3. Immunoblot analyses demonstrating effects of SC144 on IL-6/JAK-STAT3 signaling pathway. (**A**) Immunoblotting reveals robust expression of P-Stat3 in MMs from vehicle-treated control mice but diminished expression in MMs from SC144-treated mice, with expression of total Stat3 (T-Stat3) markedly reduced in tumors from mice in the 150 mg/kg SC144-treatment group. (**B**) SC144 inhibits activation of Stat3 by IL-6 in non-malignant mesothelial cells (NMC) from *Nf2*$^{+/-}$*;Cdkn2a*$^{+/-}$ mice. Early passage (p. 4) *Nf2*$^{+/-}$*;Cdkn2a*$^{+/-}$ NMC 701 and 704 were cultured overnight in medium containing 1% FBS containing 40 μM SC144. The following morning, the medium was replenished with fresh SC144 for another 4 h, and then IL-6 at 100 ng/ml was added for the final 15 min before harvesting cells to prepare lysates for immunoblot analysis. (**C**) Immunoblotting showing reduced Nf2/Merlin and p16Ink4a expression in NMC 701 and 704 (both haploinsufficient for *Nf2* and *Cdkn2a*) as compared to that of wild-type NMC (NMC wt).

of sulindac appears to be unrelated to COX inhibition, but instead involves an off-target phosphodiesterase (PDE). In human CRC cells, but not normal colonocytes, sulindac sulfide inhibits cyclic guanosine 3′,5′-monophosphate phosphodiesterase (cGMP PDE) activity, increases intracellular cyclic guanosine monophosphate phosphodiesterase (cGMP) levels, and activates cGMP-dependent protein kinase (PKG) at concentrations that inhibit cell proliferation and induce apoptosis (14). The mechanism by which sulindac sulfide and the cGMP/PKG pathway inhibited CRC cell growth was found to involve transcriptional suppression of β-catenin to inhibit Wnt/β-catenin T-cell factor transcriptional activity, leading to downregulation of cyclin D1 and survivin. Piazza et al. proposed the future development of safer and more efficacious drugs that inhibit PDE5 and PDE10, which are frequently overexpressed in various tumors and are critical for tumor cell growth (15). They suggested using a sulindac scaffold to 'design-out' COX-1/2 inhibitory activity, while selectively improving the potency to inhibit PDE5/10 to activate cGMP/PKG signaling. Recently, a novel non-COX inhibitory derivative of sulindac (ADT 061) with selective PDE10 inhibitory activity was shown to potently inhibit the growth of CRC cells that express high levels of PDE10 (14). Oral administration of ADT 061 significantly suppressed the formation of colon adenomas in a mutant *Apc* mouse model of CRC without obvious toxicity, thus providing a rationale for the development of ADT 061 for the treatment or prevention of adenomas in individuals at risk of developing CRC (14). Furthermore, DuBois et al. recently reported that simply targeting COX-2–derived PGE_2, an inflammatory mediator and tumor promoter, alone may be effective in CRC prevention and treatment. Given that EP4 antagonists have similar efficacy to celecoxib in the prevention and treatment of colorectal adenomas and CRC, the use of these agents will likely avoid serious cardiovascular side effects associated with other NSAIDs and COXIB use (16).

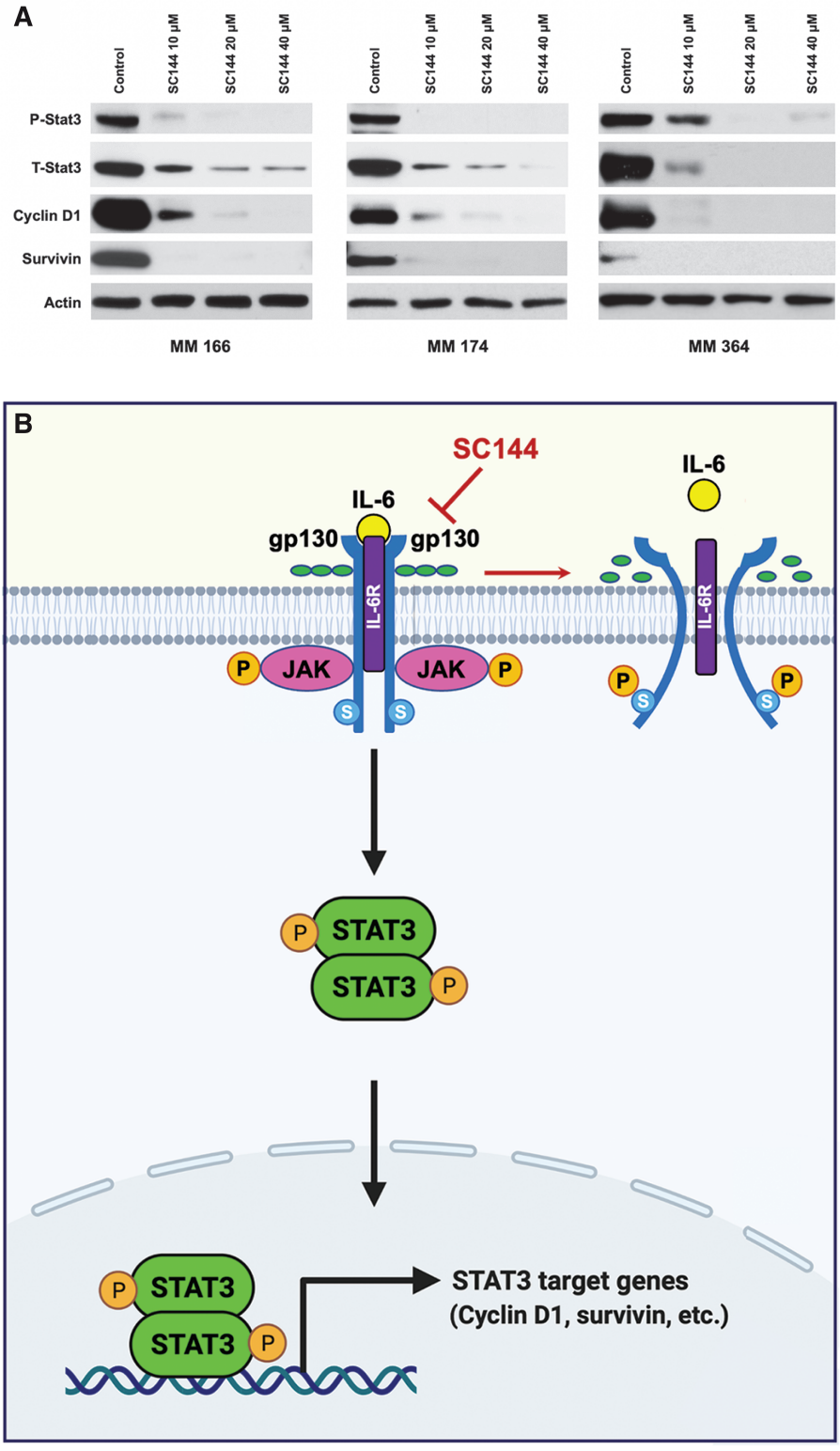

Figure 4. Effect of SC144 on STAT3 target genes. (**A**) Immunoblot analysis documenting markedly diminished expression of T-STAT and P-Stat3 with increasing dose of SC144, with a consequent abrogated expression of two Stat3 target gene products, cyclin D1 and survivin. (**B**) Cartoon depiction of the effect of SC144 on the IL-6/JAK-STAT3 signaling pathway. SC144 interferes with the IL-6-gp130-IL-6 receptor (IL-6R) interaction by binding to gp130. As a result (red arrow), SC144 induces phosphorylation (P) on Ser782 (S) of gp130 and deglycosylation (release of green oval symbols) of this transmembrane protein, as well as conformational changes and decreased activity of gp130 (8). As a result of treatment with SC144, phosphorylation and nuclear translocation of Stat3 are blocked, thereby leading to diminished expression of STAT3 target gene products, such as those involved in cell proliferation and survival (e.g. cyclin D1 and survivin). Panel (**B**) was created in part with Biorender.com software.

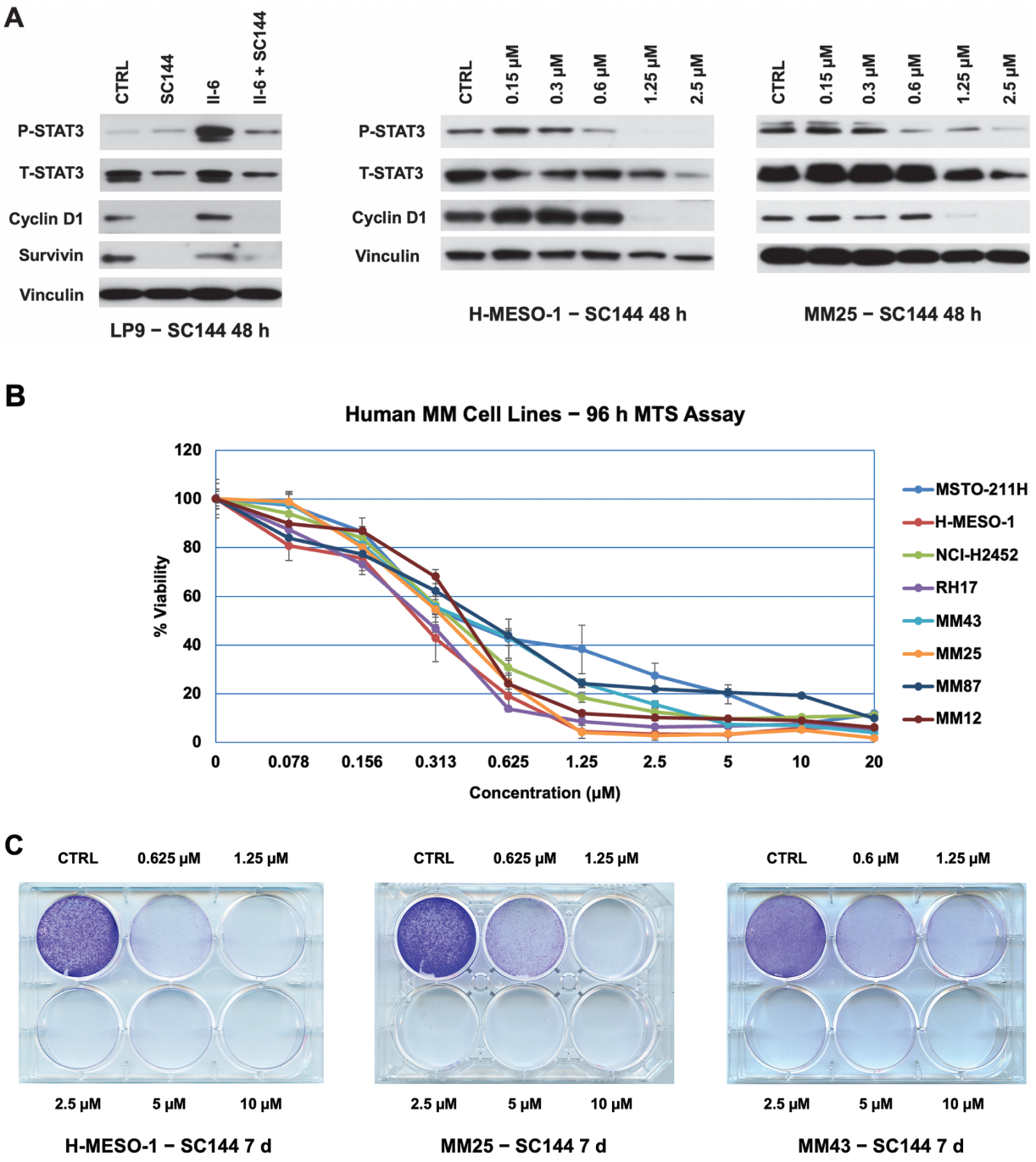

Figure 5. Effects of SC144 on human mesothelial cells and MM cell lines. (**A**) Immunoblot analyses demonstrating effects of SC144 on IL-6/JAK-STAT3 signaling pathway. Left panel, SC144 inhibits IL-6-induced activation of STAT3 and expression of two protein products (cyclin D1 and survivin) of STAT3 target genes in LP9 mesothelial cells. The LP9 cells were cultured overnight in medium containing 1% FBS containing 10 μM SC144. The following day, the medium was replenished with fresh SC144 for another 4 h, and then IL-6 (100 ng/ml) was added for the final 15 min before harvesting cells to prepare lysates for immunoblotting. *Right two panels*, immunoblot analysis depicting the effect of SC144 on P-STAT3, T-STAT3 and cyclin D1 in human MM cell lines H-MESO-1 and MM25 cultured in the presence of increasing concentrations of SC144 for 48 h. Vinculin was used as a loading control. (**B**) SC144 inhibits cell viability of human MM cell lines in a dose-dependent manner. Cell viability at increasing concentrations of SC144 was assessed by MTS assay 96 h after beginning treatment. (**C**) Colony formation in human MM cell lines treated with increasing concentrations of SC144. Cells were treated with five different concentrations of SC144 for 7 days. Each experiment was performed in triplicate, and representative stained plates for each cell line are shown.

Treatment of asbestos-exposed *Nf2*$^{+/-}$;*Cdkn2a*$^{+/-}$ mice with SC144 also delayed MM development and prolonged survival compared to asbestos-exposed *Nf2*$^{+/-}$;*Cdkn2a*$^{+/-}$ mice treated with vehicle. Moreover, SC144 showed no evidence of toxicity, as there were no deaths or significant weight loss after treatment with this small-molecule inhibitor.

Interestingly, the median survival times for the control groups differed in the sulindac/anakinra chemoprevention

study (23 weeks) and the SC144 study (19.4 weeks). However, these two experiments were carried out at different times and under different conditions. For the sulindac/anakinra , the control group was injected i.p. with PBS 3 days a week, whereas for the SC144 experiment, the control group was given a thick vehicle solvent (Labrafil M 1944 in citrate buffer) by oral gavage 5 days a week. Thus, the control group animals in the SC144 experiment were likely under greater stress compared to those in the control group in the sulindac/anakinra study, which may have contributed to the shorter survival of the SC144 control group. Had SC144 been water soluble, the SC144 control group might have survived longer.

SC144 belongs to a group of hydrazide compounds that currently show promise as novel anticancer agents through the inhibition of gp130 (8). Gp130 serves as a hub for the receptor-signaling complex of eight cytokines (IL-6, IL-11, IL-27, LIF, CNTF, OSM, CT-1 and CLC). Ligand binding induces the association of gp130 with specific cytokine receptors, followed by the activation of downstream signaling cascades, including the JAK/STAT, RAS/RAF/MAPK and PI3K/AKT pathways (17–23). Among these cascades, gp130/IL-6/STAT3 signaling has been the most well-studied because of the critical roles of IL-6 and STAT3 in inflammation-associated tumorigenesis (18). As an inflammatory cytokine, IL-6 orchestrates chemokine-directed leukocyte trafficking and directs the transition from innate to adaptive immunity by regulating leukocyte activation, differentiation and proliferation (18). STAT3 activity often correlates with tumorigenesis and is associated with malignant growth, survival, angiogenesis and metastasis, each of which has been linked to gp130 signaling (18,24).

Asbestos induces the release of pro-inflammatory cytokines such as IL-6, which play a critical role in the formation of MM. IL-6 is a component of the JAK-STAT3 pathway that contributes to inflammation-associated tumorigenesis. Our *in vitro* studies confirmed that the small-molecule gp130 inhibitor SC144 targets the IL-6/JAK-STAT3 signaling pathway. SC144 markedly diminished the expression of phosphorylated (active) STAT3 in a dose-dependent manner and, as expected, inhibited the activation of STAT3 by IL-6 (Figure 3). By inhibiting the interaction of gp130 with the IL-6 receptor, SC144 would blunt signaling from the IL-6/JAK-STAT3 pathway and abolish the expression of two known downstream effectors, cyclin D1 and survivin (Figure 4). This supports the idea that SC144 restrains MM cell proliferation and blocks a key inhibitor of apoptosis, which together are proposed to contribute, in part, to the delayed onset of MM observed with SC144 treatment.

There are known links between IL-6/STAT3 and MM that suggest that further development of gp130 inhibitors would have translational relevance in MM. For example, in one study, activated tyrosine-phosphorylated STAT3 was found in 27/44 (61.4%) archived pleural MM cases (25). In another report, MM patients were found to have large amounts of IL-6 in the pleural fluid that leak into the systemic circulation and induce clinical inflammatory reactions (26). Moreover, within the MM tumor microenvironment, IL-6 is thought to play a prominent role in the malignant phenotype as manifested through STAT signaling (27). In addition, *in vitro* studies have demonstrated high phospho (P)-STAT3 levels in human MM cell lines H2052, H2452 and 211H, and *STAT3* siRNA treatment of these cells induced apoptosis and decreased cell proliferation (28).

As inflammation plays a key role in the pathogenesis of numerous malignancies, gp130/IL-6/STAT3 signaling is elevated in many human cancers (e.g. colon, lung, breast and pancreas) (29). Both non-phosphorylated inactive cytoplasmic STAT3, which promotes cell motility and tumor invasion, and the phosphorylated active form of STAT3 (P-STAT3), which mediates its effects via nuclear transcriptional activity, are upregulated in a high percentage of MMs, making STAT3 a potentially significant target for therapeutic intervention in this disease (25). IL-6 has been shown to mediate processes such as cell proliferation and chemoresistance in MM, suggesting a role for anti-IL-6 therapeutics in combination with standard chemotherapy (27). STAT3 is thought to be required for the maintenance of cancer stem cells, and inhibitors of STAT3 were found to decrease growth and induce immune response genes in preclinical models of malignant pleural mesothelioma (MPM), supporting the role of STAT3 inhibitors as anti-MPM therapeutic agents (30).

Although gp130 is positioned at the junction of this oncogenic signaling network and is essential for its activation, currently no small-molecule inhibitors of gp130 are under clinical development. In 2013, SC144 was identified as a first-in-class, efficacious, safe and orally active inhibitor of gp130 (17). SC144 has been shown to selectively inhibit the activation of downstream signaling pathways induced by the gp30 ligands IL-6 and LIF, with no significant effects on activation by non-gp130 ligands such as IFN-γ, SDF-1α and PDGF. SC144 exhibited cytotoxicity in a panel of platinum-sensitive and platinum-resistant epithelial ovarian cancer (EOC) cells, with no significant toxicity in normal human epithelial cells (8). In a mouse xenograft model of human EOC tumors, SC144 significantly inhibited tumor growth through gp130 inhibition and induction of tumor necrosis (8). No toxicity was evident in the normal tissues. Furthermore, SC144 has shown significant *in vivo* efficacy in immunocompetent syngeneic mouse models (31). The data presented here demonstrate that SC144 has efficacy in delaying the onset and/or slowing the progression of tumors in an asbestos-induced MM model. This is consistent with asbestos-related inflammation, which plays a key role in the pathogenesis of MM.

Unfortunately, the clinical development of SC144 has been delayed because of its poor solubility and metabolic instability. Recently, one of the authors (N.N.) has undertaken an extensive medicinal chemistry lead optimization campaign to produce analogs with increased solubility and metabolic stability. Importantly, the new analogs showed favorable properties in both single- and repeat-dosing pharmacokinetic studies. As a result, a series of second-generation analogs will soon be available that are orally active, more effective, water-soluble and display desirable pharmacokinetic properties.

Notably, anakinra, the positive control drug used in this study, showed the most pronounced effect in the asbestos-exposed *Nf2*$^{+/-}$;*Cdkn2a*$^{+/-}$ mouse model, extending the median survival of mice succumbing to MM from 23 to 34 weeks ($P < 0.0001$, log-rank test). This result is remarkably similar to that reported previously by this group in the same model, treated in the same manner (median survivals: 22.6 weeks in the anakinra-treated group vs. 33.1 weeks in the vehicle-treated control group) (4). More recently, anakinra, sulindac and aspirin were used separately in a chemoprevention study in a transgenic mouse model of Barrett's esophagus and

esophageal adenocarcinoma (L2-ILIB mice), which exhibited accelerated tumor formation on a high-fat diet (HFD) (32). Notably, anakinra diminished tumor progression in L2-IL-1B mice with or without HFD, whereas both NSAIDs were effective chemopreventive agents in an accelerated HFD-fed mouse model.

Importantly, while the goal of our studies was chemoprevention of MM, all mice treated with SC144, sulindac or anakinra eventually did die of their asbestos-induced tumors. While we did observe prolonged survival with the use of these agents, no MMs were actually prevented, suggesting that our mouse model was too aggressive to detect a chemopreventive effect. The *Nf2*$^{+/-}$;*Cdkn2a*$^{+/-}$ model has heterozygous deletions of both *Nf2* and *Cdkn2a*, the latter deleting a copy of exon 2, which encodes portions of both p16Ink4a and p19Arf (p14ARF in humans). Thus, *Nf2*$^{+/-}$;*Cdkn2a*$^{+/-}$ mice start out with haploinsufficiency for three different tumor suppressor genes, and upon chronic exposure to asbestos, virtually 100% of mice develop MM, with a median survival of 19.4–23 weeks. Despite this, a significant decrease in Ki67 staining was observed in SC144-treated *Nf2*$^{+/-}$;*Cdkn2a*$^{+/-}$ mice, which suggests that treatment with this class of drug would benefit patients in a prevention setting where tumor onset is not as rapid and aggressive, e.g. where a single predisposing genetic lesion is present in an at-risk individual. Thus, in future experiments, we plan to use a less aggressive model such as *Bap1*$^{+/-}$ mice, which develop asbestos-induced MMs in 71–74% of animals with a median survival of ~45 weeks (10,33).

Our data do not allow us to distinguish with certainty between the delayed onset of MM formation and slower progression of these tumors in SC144-, sulindac- or anakinra-treated mice, although the reduced Ki67 staining in SC144-treated mice suggests that slow progression is a significant contributing factor. However, given the marked difference in Ki67 staining—indicative of cell proliferation—the survival difference between the treatment groups is unexpectedly small. This suggests that other factors, e.g. drug-related apoptotic rates, need to be considered as well in the context of the delayed growth of MMs in SC144-treated versus control mice. Regardless, the data showing that SC144 can decrease Stat3 activity and downregulate survivin and cyclin D1 expression demonstrate that this novel agent is inhibiting its intended target (i.e. the gp130–IL-6R interaction) and thereby blocking the critical downstream Stat3 signaling pathway important in MM pathogenesis.

It is also important to point out that SC144 is the first-generation inhibitor, and ongoing studies by one of us (N.N.) have led to the development of the second generation of gp130 inhibitors with more favorable solubility and PK parameters. The limited half-life combined with the once-daily treatment schedule may have contributed to the limited efficacy obtained in the studies presented here. The use of newer SC144 analogs in a less aggressive mouse model would provide more definitive data regarding the potential efficacy of gp130-IL-6-STAT3 pathway inhibition, but the results obtained in the current study still provide proof-of-principle that this class of inhibitors could prove highly efficacious for the prevention/delay and treatment of MM and possibly other cancers.

Collectively, the preclinical studies presented here have implications for individuals at a high risk of MM, such as asbestos workers. The emerging availability of newer, more potent SC144 analogs with improved PK properties presents exciting opportunities for advanced preclinical studies to support future IND filing. The resulting data will inform the design of future trials that are anticipated to benefit individuals at an elevated risk of developing this uniformly fatal disease.

Supplementary material

Supplementary data are available at Carcinogenesis online.

Funding

This work was funded by the National Institutes of Health (Task Order #HHSN261201500032I/HHSN26100003 to J.R.T., contract #HHSN26120018000026I to J.M.W. and grant number CA06927 to Fox Chase Cancer Center). The following Fox Chase Cancer Center core services assisted in this project: Laboratory Animal, Histopathology, Cell Culture, Biostatistics and Bioinformatics Facilities.

Conflict of Interest Statement: J.R.T. has a patent on *BAP1* mutation testing and has provided legal consultation regarding the role of genetic alterations in malignant mesothelioma. The remaining authors declare no conflicts of interest. The research was performed in the absence of any commercial or financial relationships that could be construed as a potential conflict of interest.

Data availability

The data underlying this article are available in the article and in its online supplementary material. Any additional details concerning the methodology or data in the report will be shared on reasonable request to the corresponding author.

References

1. Berry, T.A. et al. (2022) Asbestos and other hazardous fibrous minerals: potential exposure pathways and associated health risks. *Int. J. Environ. Res. Public Health*, 19, 4031.
2. Carbone, M. et al. (2019) Mesothelioma: scientific clues for prevention, diagnosis, and therapy. *CA Cancer J. Clin.*, 69, 402–429.
3. Testa, J.R. et al. (2020) Preclinical models of malignant mesothelioma. *Front. Oncol.*, 10, 101.
4. Kadariya, Y. et al. (2016) Inflammation-related IL1beta/IL1R signaling promotes the development of asbestos-induced malignant mesothelioma. *Cancer Prev. Res.*, 9, 406–414.
5. Pietrofesa, R.A. et al. (2016) Flaxseed lignans enriched in secoisolariciresinol diglucoside prevent acute asbestos-induced peritoneal inflammation in mice. *Carcinogenesis*, 37, 177–187.
6. Dostert, C. et al. (2008) Innate immune activation through Nalp3 inflammasome sensing of asbestos and silica. *Science*, 320, 674–677.
7. Menges, C.W. et al. (2014) Tumor suppressor alterations cooperate to drive aggressive mesotheliomas with enriched cancer stem cells via a p53-miR-34a-c-Met axis. *Cancer Res.*, 74, 1261–1271.
8. Xu, S. et al. (2013) Discovery of a novel orally active small-molecule gp130 inhibitor for the treatment of ovarian cancer. *Mol. Cancer Ther.*, 12, 937–949.
9. Grande, F. et al. (2007) Synthesis and antitumor activities of a series of novel quinoxalinhydrazides. *Bioorg. Med. Chem.*, 15, 288–294.
10. Xu, J. et al. (2014) Germline mutation of *Bap1* accelerates development of asbestos-induced malignant mesothelioma. *Cancer Res.*, 74, 4388–4397.

11. Cheng, J.Q. et al. (1999) Frequent mutations of *NF2* and allelic loss from chromosome band 22q12 in malignant mesothelioma: evidence for a two-hit mechanism of *NF2* inactivation. *Genes Chromosomes Cancer*, 24, 238–242.
12. Fajardo, A.M. et al. (2015) Chemoprevention in gastrointestinal physiology and disease. Anti-inflammatory approaches for colorectal cancer chemoprevention. *Am. J. Physiol. Gastrointest. Liver Physiol.*, 309, G59–G70.
13. Neuhann, T.M. et al. (2022) Long-term chemoprevention in patients with adenomatous polyposis coli: an observational study. *Fam. Cancer*, 21, 463–472.
14. Lee, K.J. et al. (2021) Suppression of colon tumorigenesis in mutant *Apc* mice by a novel PDE10 inhibitor that reduces oncogenic beta-catenin. *Cancer Prev. Res.*, 14, 995–1008.
15. Piazza, G.A. et al. (2020) PDE5 and PDE10 inhibition activates cGMP/PKG signaling to block Wnt/beta-catenin transcription, cancer cell growth, and tumor immunity. *Drug Discov. Today*, 25, 1521–1527.
16. Wei, J. et al. (2022) The COX-2-PGE2 pathway promotes tumor evasion in colorectal adenomas. *Cancer Prev. Res.*, 15, 285–296.
17. Xu, S. et al. (2013) gp130: a promising drug target for cancer therapy. *Expert Opin Ther. Targets*, 17, 1303–1328.
18. Jones, S.A. et al. (2018) Recent insights into targeting the IL-6 cytokine family in inflammatory diseases and cancer. *Nat. Rev. Immunol.*, 18, 773–789.
19. Taher, M.Y. et al. (2018) The role of the interleukin (IL)-6/IL-6 receptor axis in cancer. *Biochem. Soc. Trans.*, 46, 1449–1462.
20. Kang, S. et al. (2019) Targeting interleukin-6 signaling in clinic. *Immunity*, 50, 1007–1023.
21. Azar, W.J. et al. (2020) Noncanonical IL6 signaling-mediated activation of YAP regulates cell migration and invasion in ovarian clear cell cancer. *Cancer Res.*, 80, 4960–4971.
22. Omokehinde, T. et al. (2020) GP130 cytokines in breast cancer and bone. *Cancers*, 12, 326.
23. Uciechowski, P. et al. (2020) Interleukin-6: a masterplayer in the cytokine network. *Oncology*, 98, 131–137.
24. Johnson, D.E. et al. (2018) Targeting the IL-6/JAK/STAT3 signalling axis in cancer. *Nat. Rev. Clin. Oncol.*, 15, 234–248.
25. Achcar Rde, O. et al. (2007) Expression of activated and latent signal transducer and activator of transcription 3 in 303 non-small cell lung carcinomas and 44 malignant mesotheliomas: possible role for chemotherapeutic intervention. *Arch. Pathol. Lab. Med.*, 131, 1350–1360.
26. Nakano, T. et al. (1998) Interleukin 6 and its relationship to clinical parameters in patients with malignant pleural mesothelioma. *Br. J. Cancer*, 77, 907–912.
27. Abdul Rahim, S.N. et al. (2015) The role of interleukin-6 in malignant mesothelioma. *Transl. Lung Cancer Res.*, 4, 55–66.
28. Dabir, S. et al. (2014) Low PIAS3 expression in malignant mesothelioma is associated with increased STAT3 activation and poor patient survival. *Clin. Cancer Res.*, 20, 5124–5132.
29. Gharibi, T. et al. (2020) Targeting STAT3 in cancer and autoimmune diseases. *Eur. J. Pharmacol.*, 878, 173107.
30. Lapidot, M. et al. (2020) Inhibitors of the transcription factor STAT3 decrease growth and induce immune response genes in models of malignant pleural mesothelioma (MPM). *Cancers*, 13, 7.
31. Lu, T. et al. (2020) Up-regulation of hypoxia-inducible factor antisense as a novel approach to treat ovarian cancer. *Theranostics*, 10, 6959–6976.
32. Baumeister, T. et al. (2021) Anti-inflammatory chemoprevention attenuates the phenotype in a mouse model of esophageal adenocarcinoma. *Carcinogenesis*, 42, 1068–1078.
33. Kadariya, Y. et al. (2016) Bap1 is a bona fide tumor suppressor: genetic evidence from mouse models carrying heterozygous germline Bap1 mutations. *Cancer Res.*, 76, 2836–2844.